



Research article

The role of cuproptosis-related genes in pan-cancer and the development of cuproptosis-related risk model in colon adenocarcinoma

Chunwei Li^{a,j,1}, Lili Zhu^{a,1}, Qinghua Liu^a, Mengle Peng^{b,1}, Jinhai Deng^c, Zhirui Fan^d, Xiaoran Duan^a, Ruyue Xue^a, Zhiping Guo^e, Xuefeng Lv^f, Lifeng Li^{a,g,h,i,**}, Jie Zhao^{a,j,*}

^a National Engineering Laboratory for Internet Medical Systems and Applications, The First Affiliated Hospital of Zhengzhou University, Zhengzhou, 450052, Henan, China

^b Department of Clinical Laboratory, Henan No.3 Provincial People's Hospital, Zhengzhou, 450006, Henan, China

^c Clinical Research Center (CRC), Medical Pathology Center (MPC), Cancer Early Detection and Treatment Center (CEDTC), Translational Medicine Research Center (TMRC), Chongqing University Three Gorges Hospital, Chongqing University, Wanzhou, Chongqing, China

^d Department of Integrated Traditional and Western Medicine, The First Affiliated Hospital of Zhengzhou University, Zhengzhou University, Zhengzhou, 450052, Henan, China

^e Fuwai Central China Cardiovascular Hospital, Zhengzhou, 450052, Henan, China

^f Department of Clinical Laboratory, The Third Affiliated Hospital of Zhengzhou University, Zhengzhou, Henan, China

^g Cancer Center, The First Affiliated Hospital of Zhengzhou University, Zhengzhou, 450052, Henan, China

^h State Key Laboratory of Pathogenesis, Prevention and Treatment of High Incidence Diseases in Central Asia, Xinjiang Medical University, Urumqi, China

ⁱ Medical School, Huanghe Science and Technology University, 666 Zi Jing Shan Road, Zhengzhou, 450000, Henan, China

^j Department of Pharmacy, The First Affiliated Hospital of Zhengzhou University, Zhengzhou, 450052, Henan, China

ARTICLE INFO

Keywords:
Cuproptosis
FDX1
CDKN2A

ABSTRACT

Cancer is widely regarded as a leading cause of death in humans, with colon adenocarcinoma (COAD) ranking among the most prevalent types. Cuproptosis is a novel form of cell death mediated by protein lipoylation. Cuproptosis-related genes (CRGs) participate in tumorigenesis and development. Their role in pan-cancer and COAD require further investigation. This study

Abbreviations: GBM, glioblastoma multiforme; OV, ovarian serous cystadenocarcinoma; UCEC, uterine corpus endometrial carcinoma; BLCA, bladder urothelial carcinoma; ESCA, esophageal carcinoma; KICH, kidney chromophobe; (LICH, liver hepatocellular carcinoma; LUSC, lung squamous cell carcinoma; LUAD, lung adenocarcinoma; STAD, stomach adenocarcinoma; BRCA, breast carcinoma; COAD, colon adenocarcinoma; HNSC, head and neck squamous cell carcinoma; KIRC, kidney renal clear cell carcinoma; PRAD, prostate adenocarcinoma; KIRP, kidney renal papillary cell carcinoma; THCA, thyroid carcinoma; TGCT, testicular germ cell tumours; PAAD, pancreatic adenocarcinoma; CESC, cervical squamous cell carcinoma and endocervical adenocarcinoma; SARC, sarcoma; THYM, thymoma; MESO, mesothelioma; CHO, Lcholangiocarcinoma; READ, rectum adenocarcinoma; SKCM, skin cutaneous melanoma; LGG, brain lower grade glioma; DLBC, lymphoid neoplasm diffuse large B-cell lymphoma; UCS, uterine carcinosarcoma; ACC, adrenocortical carcinoma; PCPG, pheochromocytoma and paraganglioma; UVM, uveal melanoma; LAML, acute myeloid leukemia.

* Corresponding author. National Engineering Laboratory for Internet Medical Systems and Applications, The First Affiliated Hospital of Zhengzhou University, Zhengzhou, 450052, Henan, China.

** Corresponding author. National Engineering Laboratory for Internet Medical Systems and Applications, The First Affiliated Hospital of Zhengzhou University, Zhengzhou, 450052, Henan, China.

E-mail addresses: lilifeng0317@163.com (L. Li), jiezhao2016@163.com (J. Zhao).

¹ These authors contributed equally to this work.

<https://doi.org/10.1016/j.heliyon.2024.e34011>

Received 4 March 2024; Received in revised form 30 May 2024; Accepted 2 July 2024

Available online 2 July 2024

2405-8440/© 2024 The Authors. Published by Elsevier Ltd. This is an open access article under the CC BY-NC-ND license (<http://creativecommons.org/licenses/by-nc-nd/4.0/>).

LIPT1
Pan-cancer
Colon adenocarcinoma

comprehensively evaluated the relationship among CRGs, pan-cancer, and COAD. Our research revealed the differential expression of CRGs and the cuproptosis potential index (CPI) between normal and tumour tissues, and further explored the correlation of CRGs or CPI with prognosis, immune infiltration, tumor mutant burden (TMB), microsatellite instability (MSI), and drug sensitivity in pan-cancer. Gene set enrichment analysis (GSEA) revealed that oxidative phosphorylation and fatty acid metabolism pathways were significantly enriched in the high CPI group of most tumours. FDX1 and CDKN2A were chosen for further exploration, and we found an independent association between FDX1 and CDKN2A and prognosis, immune infiltration, TMB, and MSI in pan-cancer. Furthermore, a prognostic risk model based on the association between CRGs and COAD was built, and the correlations between the risk score and prognosis, immune-related characteristics, and drug sensitivity were analysed. COAD was then divided into three subtypes using cluster analysis, and the differences among the subtypes in prognosis, CPI, immune-related characteristics, and drug sensitivity were determined. Due to the level of LIPT1 was notably positive related with the risk score, the cytological identification was carried out to identify the association of LIPT1 with proliferation and migration of colon cancer cells. In summary, CRGs can be used as potential prognostic biomarkers to predict immune infiltration levels in patients with pan-cancer. In addition, the risk model could more accurately predict the prognosis and immune infiltration levels of COAD and better guide the direction of clinical medication. Thus, FDX1, CDKN2A, and LIPT1 may serve as prospective new targets for cancer therapy.

1. Introduction

Cancer is the leading cause of death and a significant economic burden worldwide [1,2]. Globally, there were approximately 23.6 million new cancer cases and 10 million deaths from cancer in 2019, with increases of 26.3 % and 20.9 %, respectively, from 2010 to 2019 [3]. Colon adenocarcinoma (COAD) is one of the most common cancers worldwide, along with lung, liver, and breast cancers. Neoadjuvant chemotherapy, radiotherapy, immunotherapy, and targeted therapy have shown strong anticancer effects in clinical practice [4–7]. While advancements in treatment options and early screening have contributed to a gradual decrease in the mortality rate of COAD, unfortunately, the incidence of COAD continues to rise [8,9]. In addition, drug resistance and cancer metastasis pose many challenges in developing effective cancer treatments. Therefore, identifying more effective therapeutic targets for early detection and prognosis prediction is important to improve the prognosis of patients with cancer.

Cuproptosis, a novel form of cell death discovered by Tsvetkov et al., and cell death is induced by intracellular copper [10,11]. The mechanism of cuproptosis involves the binding of excess intracellular copper to fatty acylated proteins in the tricarboxylic acid (TCA) cycle within the mitochondria. These lipoylated copper-bound proteins aggregate and the Fe-S cluster protein is downregulated, triggering proteotoxic stress and eventual cell death [10,12–14]. Copper is an indispensable cofactor and its homeostasis is essential for many physiological reactions. Dysregulation of intracellular copper bioavailability can lead to oxidative stress and cytotoxicity [15, 16]. One study showed that cuproptosis-related cell death is mainly achieved by enhancing reactive oxygen species (ROS) levels, which makes cancer cells more susceptible to increased oxidative stress [17]. Studies have shown that cuproptosis-related genes (CRGs) can predict the prognosis and immune cell infiltration in various cancers, including renal clear cell carcinoma, hepatocellular carcinoma, soft tissue sarcomas, melanoma, osteosarcoma, head and neck squamous cell carcinoma, glioma and lung adenocarcinoma [18–30]. Currently, there is a lack of pertinent literature available to study the connection between CRGs and their impact on pan-cancer and specifically COAD.

In the present study, we comprehensively analysed the mRNA levels of ten CRGs (FDX1, LIPT1, LIAS, DLD, PDHA1, PDHB, DLAT, MTF1, GLS, and CDKN2A) and investigated the correlation of CRGs or cuproptosis potential index (CPI) with prognosis, immune infiltration, TMB, MSI, and drug sensitivity. Furthermore, the association between the expression of CRGs and gene methylation, pathway enrichment analysis of the ten CRGs, and the mutational landscape (including CNV and SNV) of CRGs in pan-cancer were explored. Due to the role of FDX1 and CDKN2A in some cancers have been studied, FDX1 and CDKN2A were chosen for further exploration to analyse the association between FDX1 and CDKN2A and prognosis, immune infiltration, TMB, and MSI in pan-cancer. Besides, we constructed a prognostic risk model and investigated the association between the risk score and prognosis, immune cell infiltration, immune checkpoint expression, and drug sensitivity in COAD. COAD was then divided into three subtypes using cluster analysis, and the differences among the subtypes in prognosis, CPI, immune-related characteristics, and drug sensitivity were determined. Finally, we verified the association of genes in the risk model with the proliferation and migration of colon cancer cells in vitro.

In conclusion, CRGs can be used as prognostic biomarkers to predict immune cell infiltration levels in patients with pan-cancer. In addition, the risk model could more accurately predict the prognosis and immune infiltration levels of COAD and better guide the direction of clinical medication. Besides, FDX1, CDKN2A and LIPT1 may serve as novel targets for cancer therapy.

2. Materials and methods

2.1. Download transcriptome and clinical data

The Fragments per kilobase million (FPKM) transcriptome data including 33 cancers were downloaded from The Cancer Genome

Atlas (TCGA) database. Then, sample annotations and survival information from "<https://xenabrowser.net/datapages/>." were downloaded and collated. The CPI value was calculated using single-sample gene set enrichment analysis (and Gene Set Variation Analysis (GSVA)).

2.2. Differential expression analysis

The differential expression levels of CRGs and CPI were calculated in 14 cancers compared to normal tissues (only in 14 cancers was the number of paired normal tissues more than 10, and other cancers were excluded), including BLCA, ESCA, KICH, LICH, LUSC, LUAD, STAD, BRCA, COAD, HNSC, KIRC, PRAD, KIRP, and THCA. Wilcoxon tests were used to assess the differentially expressed CRGs and CPI in tumour tissues compared with those in normal tissues. The criteria of $|\log_2(\text{fold change})| > 2/3$ and $P < 0.05$ were regarded as statistically significant. The "pheatmap" R package was used to cluster the differential genes.

2.3. Gene set enrichment analysis and survival analysis

GSEA was carried out by using "cluster Profiler" and GSVA. The "ggplot2" is mainly used for image visualisation. The value of $-\log_{10}(\text{FDR})$ represents the relationship between the expression of the CRGs and the enrichment pathway. We considered the false discovery rate (FDR) to be < 0.05 , which was considered significant.

The "survminer" R package was used by Kaplan-Meier curves, log-rank tests, and univariate Cox proportional hazards regression to calculate the p values and hazard ratio (HR) with 95 % confidence interval (CI). HR is the hazard ratio of the high-risk group to the low-risk group. If the HR values were < 1 , the genes were considered protective, and HR values greater than 1 indicated that the gene was a risk factor.

2.4. Gene methylation and gene variation analysis

The association between the expression level of CRGs with gene methylation was assessed by Spearman correlation coefficient. The gene mutation data of patients with pan-cancer from the TCGA database was downloaded, and the variation of CNV (copy number variation) and SNV (single nucleotide variation) among distinct tumours were analysed by the "maftools" R package.

2.5. Association of CPI with TMB and MSI

Pearson correlation coefficient was used to assess the relationships between tumour mutation burden (TMB) and Microsatellite Instability (MSI) with CPI in pan-cancer patients and visualised as radar plots. The overall number of coding errors of somatic genes, base substitutions, and gene insertions or deletions per million bases was defined as the TMB. The TMB value for each tumour sample was calculated based on exome sequencing data from TCGA. MSI has been primarily discussed as a deficient mismatch repair system. Previous studies were collected to summarise MSI data across different cancers.

2.6. Immune-related characteristics and drug sensitivity analysis

Immune infiltration data according to CIBERSORT, and immune-related signature scores were calculated using ssGSEA for pancreatic cancer. The correlation between CPI and various immune-related characteristics was calculated by Spearman correlation coefficient in pan-cancer patients using the "MCPcounter" R package. The GDSC and CTRP databases were used to investigate the relationship between CRGs expression and drug sensitivity using Spearman's correlation coefficient. Image visualisation is mainly presented by the "ggplot2" R package.

2.7. Construction of risk model in COAD and ROC curves

CRGs were characterised using the LASSO Cox regression algorithm, and the selected genes were used to establish a prognostic risk model. The risk scores of all pan-cancer patients were calculated based on this formula: $\text{riskScore} = \sum_{i=1}^n \text{Coef}_i * x_i$ (Coef_i is coefficient, x_i is expression per gene). The cutoff point was the median risk score. Subsequently, we divided the pan-cancer patients into high- and low-risk groups. The Kaplan-Meier "survival" R package was used to plot the ROC curve, and the area under the curve (AUC) was used to judge the credibility of the prediction.

2.8. Immune-related characteristics and drug sensitivity analysis in COAD

Patients with COAD were divided into high- and low-risk groups based on median risk scores. The Wilcoxon test was used to analyse the differences in immune cell infiltration, immune checkpoint expression, and immune response (TIDE score) between high- and low-risk populations, and the IMgor210 immunotherapy cohort was used to validate the risk model. The R package "pRRophetic" was used to analyse the difference between the high- and low-risk group regarding chemotherapeutic drug sensitivity.

2.9. Cluster analysis and subgroups analysis

The "ConsensusClusterPlus" R package was used to divide the COAD patients into subtypes through consistent cluster analysis based on the CRGs' expression. Differences in survival, CPI, immune cell infiltration, immune checkpoint expression, and immune response between subgroups were analysed using chi-square tests.

COAD cell lines from the GDSC database were grouped according to their COAD subtypes. The drug sensitivity was compared among subgroups, and the differences in drug sensitivity were quantified using AUC by Kruskal tests.

2.10. qRT-PCR

Total RNAs were extracted using TRIzol reagent (Thermo Fisher Scientific, USA) according to the manufacturer's advised protocol. A NanoDrop spectrophotometer was used to determine the quality and quantity of the RNA samples. A PrimeScript RT reagent kit with a genomic DNA eraser (TaKaRa, Tokyo, Japan) was used for cDNA synthesis. SYBR qPCR Master Mix (TaKaRa, Tokyo, Japan) was used for qRT-PCR. The relative mRNA expression level was computed according to the $2^{-\Delta\Delta Ct}$ approach. All primers were synthesised by

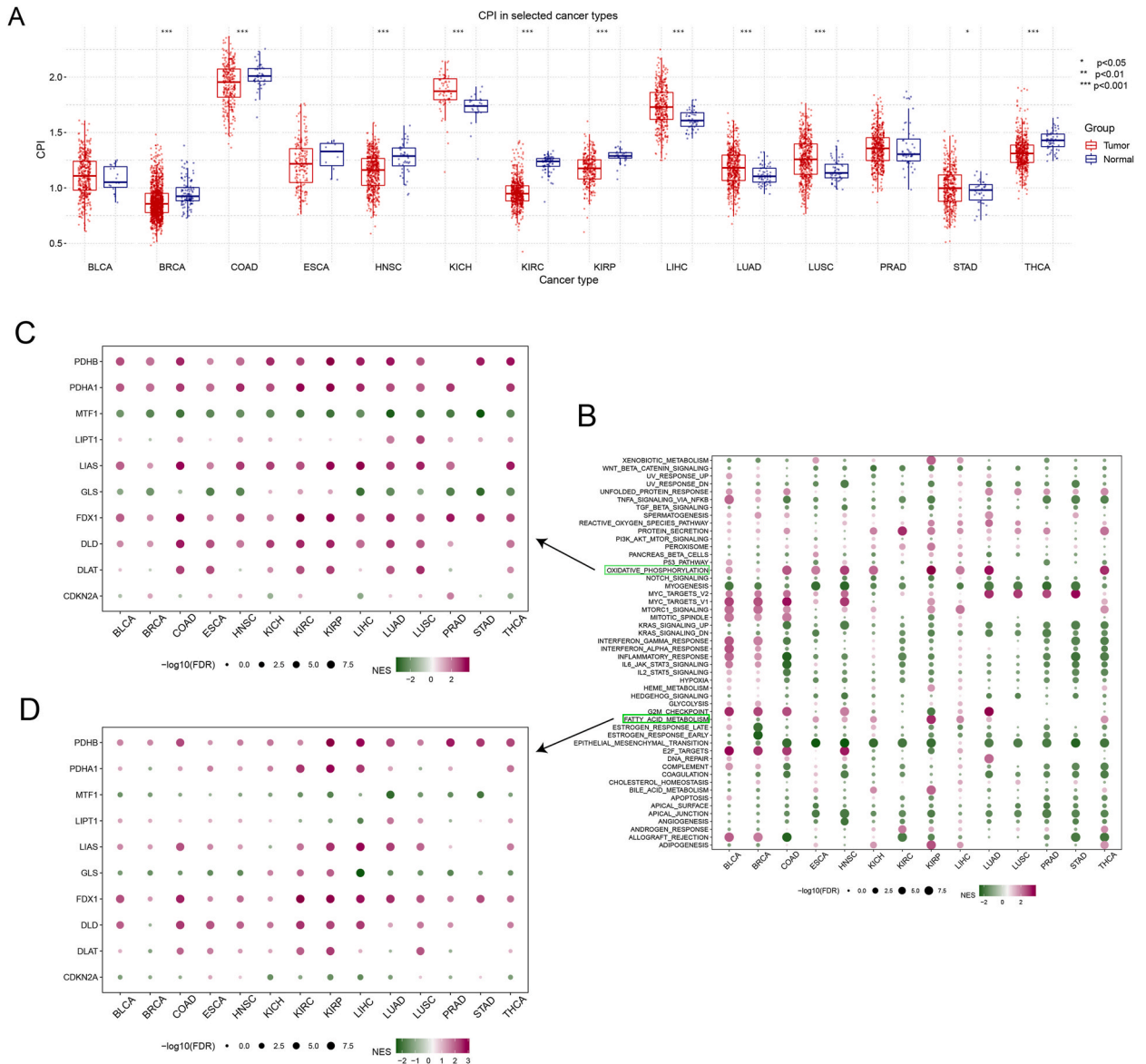


Fig. 1. CPI difference and pathway enrichment analysis of CRGs. (A) The CPI difference between normal and tumour tissues. (B) The differential expression of pathways between high and low CPI groups. (C/D) The situation of each CRGs enrichment in the two oxidative phosphorylation pathways and fatty acid metabolism, respectively. The size of the circle represents the degree of correlation.

Henan Qingke BioCompany (China). All experiments were performed in triplicates.

The primer sequences of qRT-PCR are shown in Table S1.

2.11. Transwell and clone assays

A transwell assay was used to evaluate cell migration ability. For the transwell assay, SW620, HCT116 and HT29 cells were suspended in a serum-free medium. The concentration of cells was adjusted to 2×10^5 cells/mL, and the 200 μ L cell suspension was subsequently seeded into the upper side of a transwell chamber (8 μ m pore size; Costar, Cambridge, MA). Then, 600 μ L DMEM complete

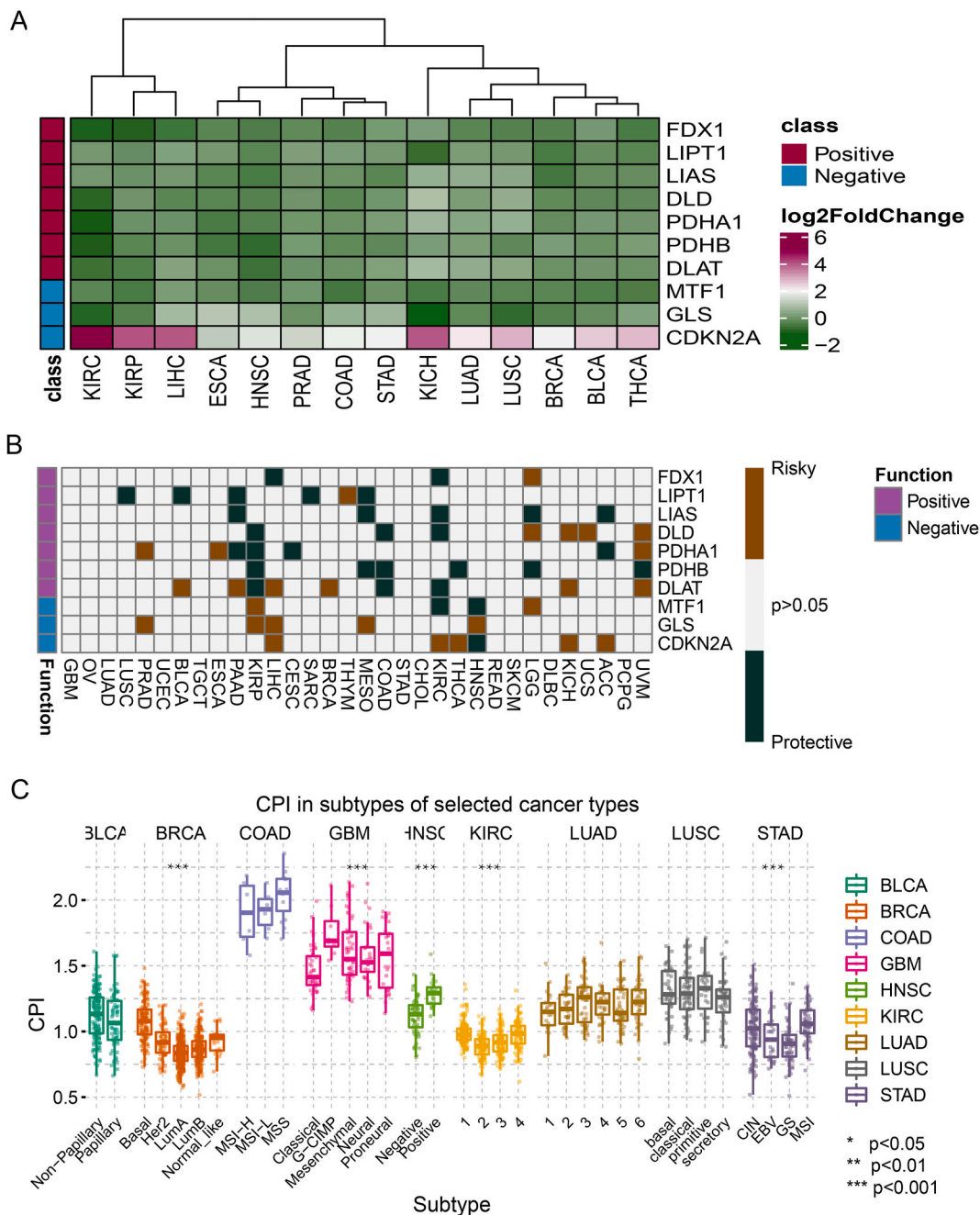


Fig. 2. Expression levels of CRGs and the association with tumour prognosis and the difference of CPI between subtypes of tumours. (A) The heatmap with expression levels of CRGs. (B) The heatmap of correlation between CRGs and tumour prognosis. (C) The difference of CPI between clinical subtypes of tumours.

medium containing 10 % FBS was added into the lower chambers. After incubation for 36h, the non-migratory cells on the upper side of the Transwell chambers were gently swabbed. Subsequently, the cells in the transwell chambers were fixed with 4 % paraformaldehyde and stained with 0.1 % crystal violet. Finally, the chambers were washed three times with PBS, air-dried, and photographed using an inverted microscope (Leica MZ8; Leica Microsystems, Wetzlar, Germany).

A clone assay was used to evaluate cell proliferative ability. For the cloning assay, the cells were suspended and counted, and 1000 cells were seeded into 6-well plates (Corning, USA), followed by 10 days of incubation. Finally, cells were fixed with 4 % paraformaldehyde and stained with 0.1 % crystal violet.

2.12. Statistical analysis

All statistical analyses were performed using R 4.1.1 and GraphPad Prism 8.0. A P-value less than 0.05 was regarded as statistically

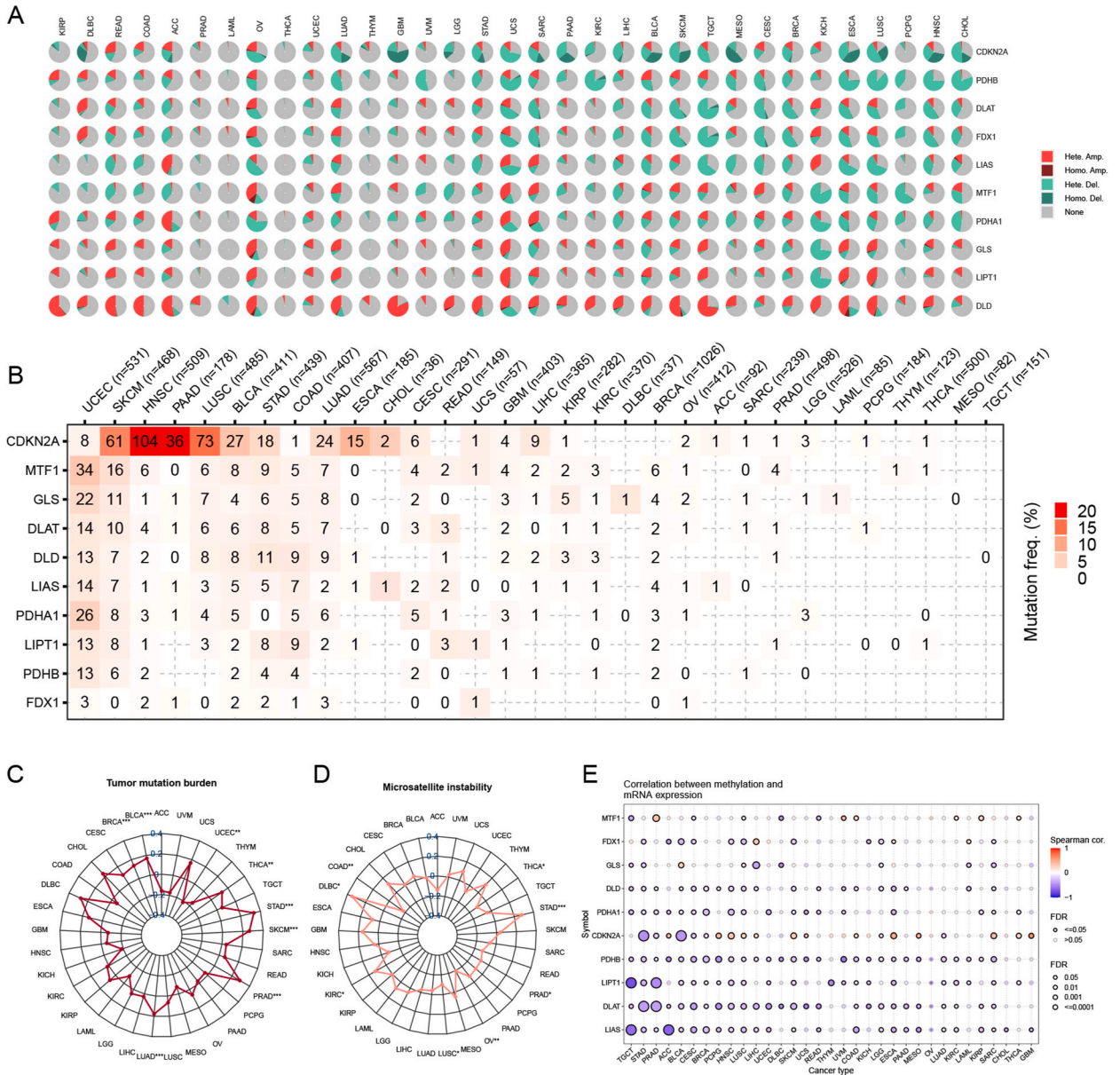


Fig. 3. Mutational landscape of CRGs and the correlation of CPI with immune variables in pan-cancer and the association of expression level with methylation of CRGs. (A) The copy number variation of CRGs in pan-cancer. (B) The single nucleotide variation of CRGs in pan-cancer. (C) Correlation of CPI with TMB in pan-cancer. (D) Association of CPI with MSI in pan-cancer. (E) Correlation between mRNA expression and methylation of CRGs.

significant, and the P -value was two-sided. The R package of "cluster Profiler" and GSVA were performed to analyse the GSEA, and FDR value < 0.05 . Wilcoxon tests were used to assess the differentially expressed CRGs and CPI in tumour tissues compared with those in normal tissues. The criteria were $|\log_2(\text{fold change})| > 2/3$ and $P < 0.05$.

3. Results

3.1. The expression level of CPI and gene set enrichment analysis based on CPI in pan-cancer

We chose tumours in which several paired normal samples from more than 10 patients, and 14 tumours satisfied the requirement and were analysed to determine the difference in CPI between normal and tumour tissues. The results showed that CPI was higher in KICH, LIHC, LUSC, LUAD, and STAD tumours and lower in BRCA, COAD, HNSC, KIRC, KIRP, and THCA tumours ($P < 0.05$) (Fig. 1A).

GSEA was performed for each tumour based on the transcriptomes of the two tumour groups with the highest 30 % and the lowest 30 % CPI to investigate the different pathways between the high and low CPI groups in the 14 tumours. We found that the oxidative phosphorylation and fatty acid metabolism pathways were significantly enriched in the high CPI group of most tumours, including ESCA, HNSC, KICH, KIRP, LIHC, LUAD, and THCA (Fig. 1B). In addition, based on the expression of CRGs, ssGSEA was performed in pan-cancer patients, and the analysis showed the situation of gene enrichment in different pathways. Two pathways, oxidative phosphorylation and fatty acid metabolism, were significantly enriched in the FDX1 and PDHB high-expression groups (Fig. 1C and D). The results showed that tumour metabolism was stronger in the high CPI group, and the expression levels of FDX1 and PDHB were positively correlated with these two pathways. However, the related mechanisms of FDX1 and PDHB metabolism need to be studied further.

3.2. Differential expression of CRGs in pan-cancer

Among the 10 CRGs, CDKN2A was highly expressed in the tumour tissues, whereas almost all the other nine genes showed low expression in the tumour groups (Fig. 2A). Previous studies have shown that FDX1 could affect the prognosis and mediate the metabolism of LUAD, and the expression of CDKN2A and FDX1 in clear cell renal cell carcinoma was also correlated with immune infiltration levels and PD-1 expression [31,32]. Thus, we focused on these two CRGs and analysed their differences in expression in the tumour groups (Figs. S1A and B). We found that the expression of FDX1 was lower in COAD, LUAD, THCA, LIHC, HNSC, KIRC, and KIRP samples than in normal samples, whereas that of CDKN2A was distinctly higher in COAD, BRCA, LUAD, THCA, LIHC, KICH, KIRC, and KIRP samples.

3.3. Relationships between CRGs with tumour prognosis and the different CPI among subtypes of tumours

By analysing the association of CRGs with tumour prognosis, we found that CRGs play different roles in the prognosis of different tumours. For example, FDX1 could serve as a protective factor in LICH and KIRC, while it is a risk factor in LGG. CDKN2A could act as a risk factor in LICH, KIRC, THCA, KICH, and ACC, while it is a protective factor in HNSC (Fig. 2B). Therefore, CRGs may serve as prognostic indicators. We obtained tumours with clinical subtypes (BLCA, BRCA, COAD, GBM, HNSC, KIRC, LUAD, LUSC, and STAD) and analysed the differences in the CPI among the tumour subtypes. We found that the CPI significantly differed among the BRCA, GBM, HNSC, KIRC, and STAD subtypes (Fig. 2C).

3.4. The mutational landscape of CRGs in pan-cancer

We analysed 33 types of tumours to identify the CNV levels in the CRGs. We found that CDKN2A, PDHB, and other genes have a large proportion of copy number deletions in various cancers and that DLD has a large degree of copy number amplification in almost all cancers. In addition, each CRG had many amplified copies in OV, UCS, and LUAD (Fig. 3A). We analysed 10088 cancer patients, including 31 types of tumours, to identify the level of single nucleotide variation and found that CDKN2A was mutated at a higher frequency in tumours (SKCM, HNSC, PAAD, and LUSC), whereas in UCEC, CRGs were all mutated to some extent (Fig. 3B).

3.5. Correlation of CRGs with TMB and MSI in pan-cancer

TMB and MSI can predict the effects of immunotherapy in clinical settings. The higher the TMB and MSI values, the better the effect of immunotherapy. Thus, in this study, we analysed the association of CPI with TMB and MSI to predict the therapeutic direction. The radar chart shows that CPI is positively correlated with TMB in BRCA, BLCA, STAD, SKCM, PRAD, and LUAD, but is negatively associated with TMB in UCEC (Fig. 3C); CPI is positively correlated with MSI in STAD, KIRC, and DLBC, while it is negatively correlated with MSI in THCA, PRAD, OV, LUSC, and COAD (Fig. 3D). We also analysed the relationship of FDX1 and CDKN2A with TMB and MSI and found that FDX1 was significantly associated with TMB and MSI in DLBC and STAD (Fig. S2A). In the ACC, CDKN2A had a significant positive correlation with TMB, and CDKN2A had a positive correlation with MSI in KICH (Fig. S2B).

3.6. Association between mRNA expression and methylation of CRGs

As shown in Fig. 3E, in most cancers, CRG expression is negatively correlated with methylation. For example, the expression of

LIPT1, LIAS, CDKN2A, and DLAT negatively correlated with methylation in TGCT, PRAD, TGCT, ACC, STAD, BLCA, STAD, and PRAD.

3.7. Correlation of CRGs with immune-related features in pan-cancer

According to previous studies, we have known that the relationship of CRGs with immune infiltration has been researched in many tumours, such as osteosarcoma, hepatocellular carcinoma, HNSC, soft tissue sarcoma, KIRC, glioma, and cutaneous melanoma [22–27, 29]. Therefore, we also analysed the association between CPI and immune infiltration in pan-cancers. We found that CPI had a negative correlation with immune-related features such as infiltration score, CD4+ T, NK, gammadelta, Tfh, and CD8+ T, but a positive correlation with immune-related features such as nTreg, effector memory, neutrophil, Th1, and DC in pan-cancer (Fig. 4A). We further investigated the relationship between FDX1 and CDKN2A and immune infiltration in pan-cancer. Obtaining the data according to CIBERSORT, we found that in most cancers, FDX1 was positively interrelated with regulatory T cells (Fig. S3A); CDKN2A was positively associated with memory CD4+ T cell resting (Fig. S3B).

3.8. Correlation between CRGs and drug sensitivity

We obtained the TOP30 drugs from the GDSC database and found that CDKN2A was positively correlated with almost all drug susceptibilities, such as Bleomycin, PD-0332991, Nutlin-3a(-), whereas LIAS, PDHB, and GLS were negatively correlated with drug sensitivity, mainly including Nutlin-3a(-) and CEP-701 (Fig. 4B). Among the TOP30 drugs obtained from the CTRP database, we found that LIAS was significantly negatively associated with almost all drug sensitivities; MK-1775, tivantinib, COL-3, and other CRGs (including LIPT1, LIAS, DLD, PDHB, DLAT, MTF1, and CDKN2A) were also negatively correlated with almost all drug sensitivities (Fig. 4C). Therefore, CRG expression of CRGs can predict the direction of clinical medication.

3.9. Established a prognostic risk model in COAD based on CRGs

COAD is one of the leading cancers worldwide, and its incidence is high at present; however, no relevant article has been published on the correlation of CRGs with COAD. Therefore, we developed a risk model to investigate the relationship between CRGs and prognosis, immune-related characteristics, and drug sensitivity. Genes were screened by utilising LASSO Cox regression (Fig. 5A), and

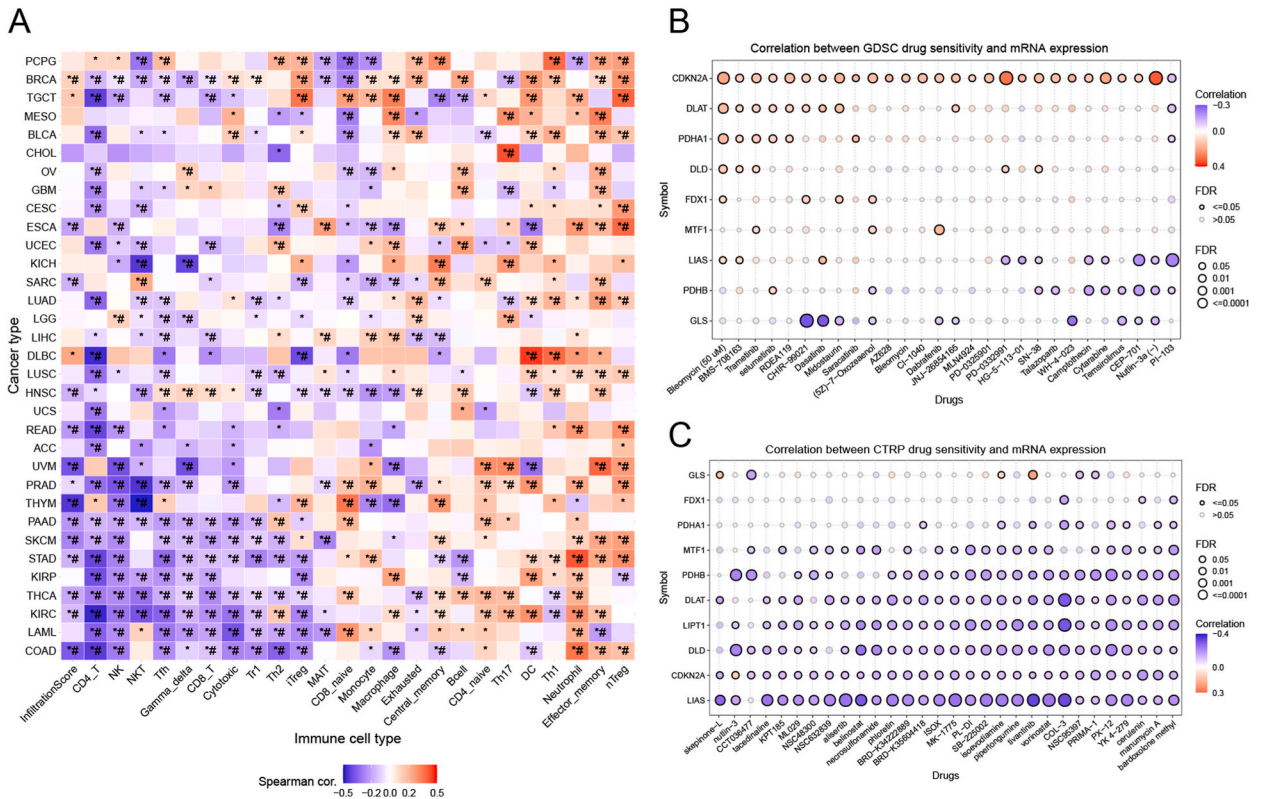


Fig. 4. Correlation of CPI with immune-related features in pan-cancer and relationship of CRGs with drug sensitivity in GDSC and CTRP database. (A) Association of CPI with immune-related features in pan-cancer. (B) Correlation of CRGs and drug sensitivity in GDSC database. (C) Relationship of CRGs and drug sensitivity in CTRP database.

the partial likelihood deviance curve was plotted versus $\log(\lambda)$ (Fig. 5B). Finally, four key CRGs were identified to build the risk model and calculate the risk score of patients with COAD according to the following algorithm: risk score = $(0.1345) \times LIPT1 + (-0.075) \times PDHB + (-0.315) \times DLAT + (0.1208) \times CDKN2A$. Fig. 5C shows the relationship between the risk score and survival status. The top represents the scatter plot of the risk score from low to high, and different colours represent different risk groups; the middle represents the scatter plot of the association of the risk score with survival time and survival status, indicating that the risk score is negatively correlated with survival time and survival status. The bottom is a heatmap that represents the situation of gene expression contained in the risk model. The protective CRGs have a higher expression, whereas the risky CRGs have a lower expression in the low-score group. KM survival curves were plotted, in which the different groups were tested using the log-rank test, and the OS was shorter in the high-risk group than in the low-risk group (Fig. 5D). The ROC curves of the risk model at 1, 3, and 5 years were drawn, and the AUC values

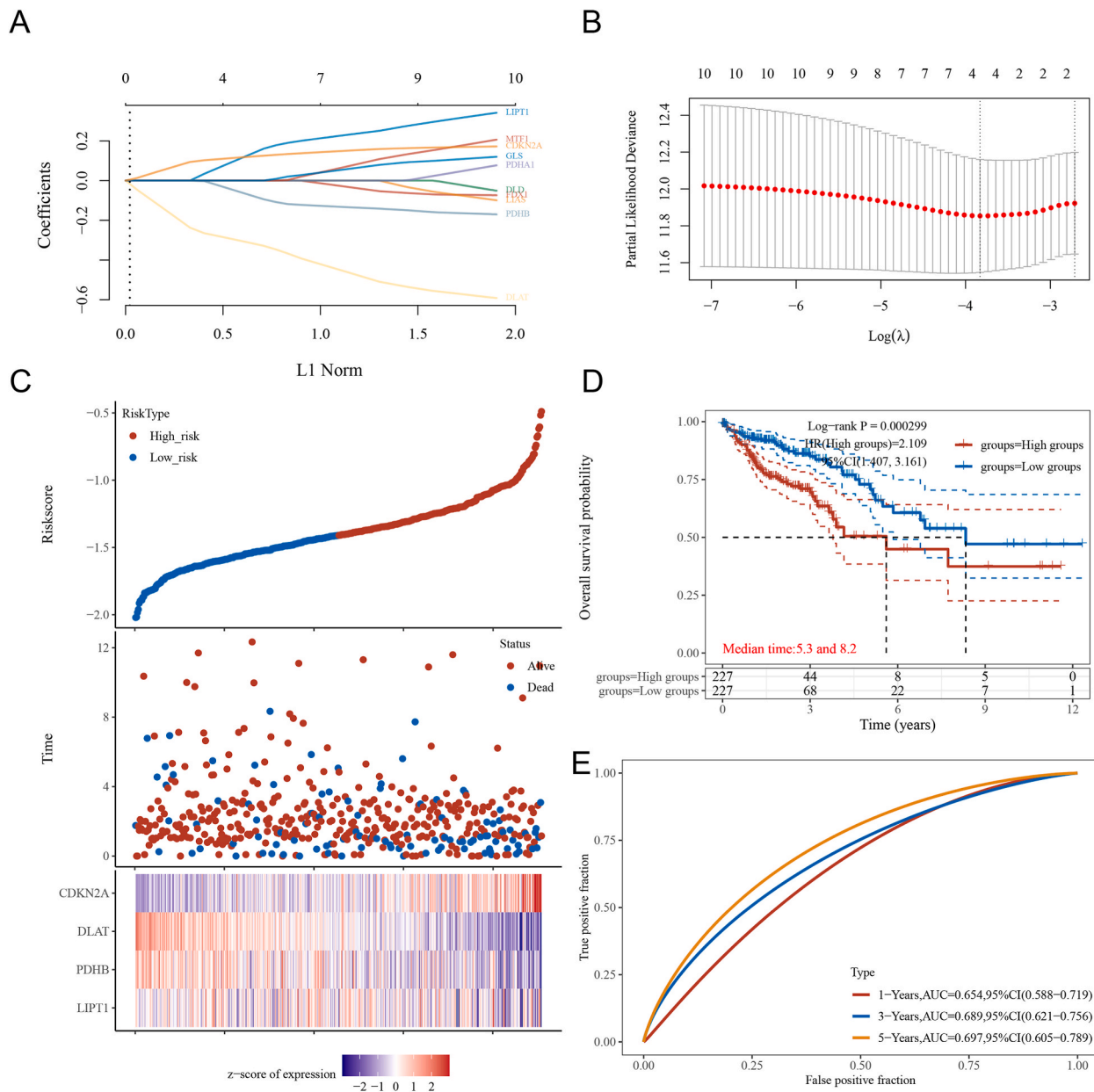


Fig. 5. A prognostic risk model was established in COAD. (A) The LASSO Cox regression for ten CRGs. (B) The partial likelihood deviance curve versus $\log(\lambda)$. (C) The top represents the scatter plot of the risk score from low to high, and different colours represent different risk groups; the middle represents the scatter plot of about the association of the risk score with survival time and survival status; the bottom is a heatmap that represents the situation of gene expression contained in the risk model. (D) KM survival curves in high- and low-risk score groups. (E) The ROC curves of the risk model at 1, 3, and 5 years. (For interpretation of the references to colour in this figure legend, the reader is referred to the Web version of this article.)

were 0.654, 0.689, and 0.697, respectively, indicating that the accuracy of the risk model was higher (Fig. 5E).

3.10. Correlation of risk score with immune signatures

Immune cell infiltration in COAD was calculated using QUANTISEQ software. It was found that the infiltration of Macrophage M1, Neutrophil, T cell CD4+(non-regulatory), and T cell regulatory (Tregs) in the high-risk group was lower than those in the low-risk group (Fig. 6A). Among the different expression levels of immune checkpoints, SIGLEC15 was significantly overexpressed in the high-risk group and CD274 (PD-L1) was significantly overexpressed in the low-risk group (Fig. 6B).

The response of the risk model to immunotherapy was evaluated using the TIDE website, and the outcomes showed that the TIDE score was higher in the high-risk group, indicating that this group was more sensitive to immunotherapy (Fig. 6C). We then used the IMvigor210 immunotherapy cohort to validate the predictive effect of immunotherapy using this risk model. The results indicated that the high-risk group patients had longer OS in the IMvigor210 cohort, showing that patients in the high-risk group could improve outcomes with immunotherapy (Fig. 6D). The CR/PR ratio was higher in the high-risk group than in the low-risk group (Fig. 6E).

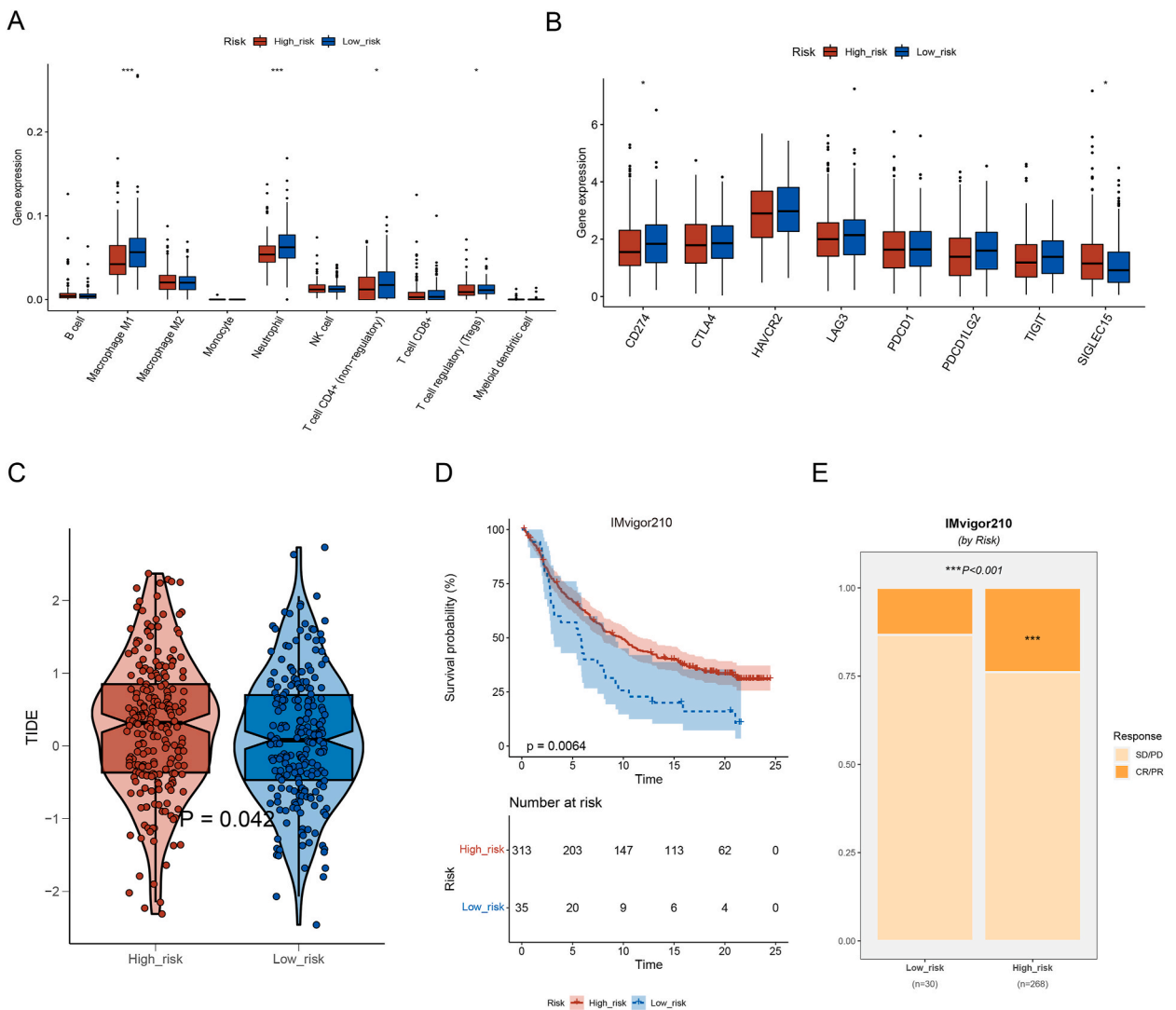


Fig. 6. Correlation between risk score and immune signatures. (A)The difference in immune cell infiltration in the high- and low-risk groups. (B) The different expressions of immune checkpoints in the high- and low-risk groups. (C) The result of the TIDE score in the high- and low-risk groups. (D) The predictive effect of immunotherapy. (E) the ratio of CR/PR in the high- and low-risk groups. (CR: complete response, PR: partial response, SD: stable disease, PD: progressive disease).

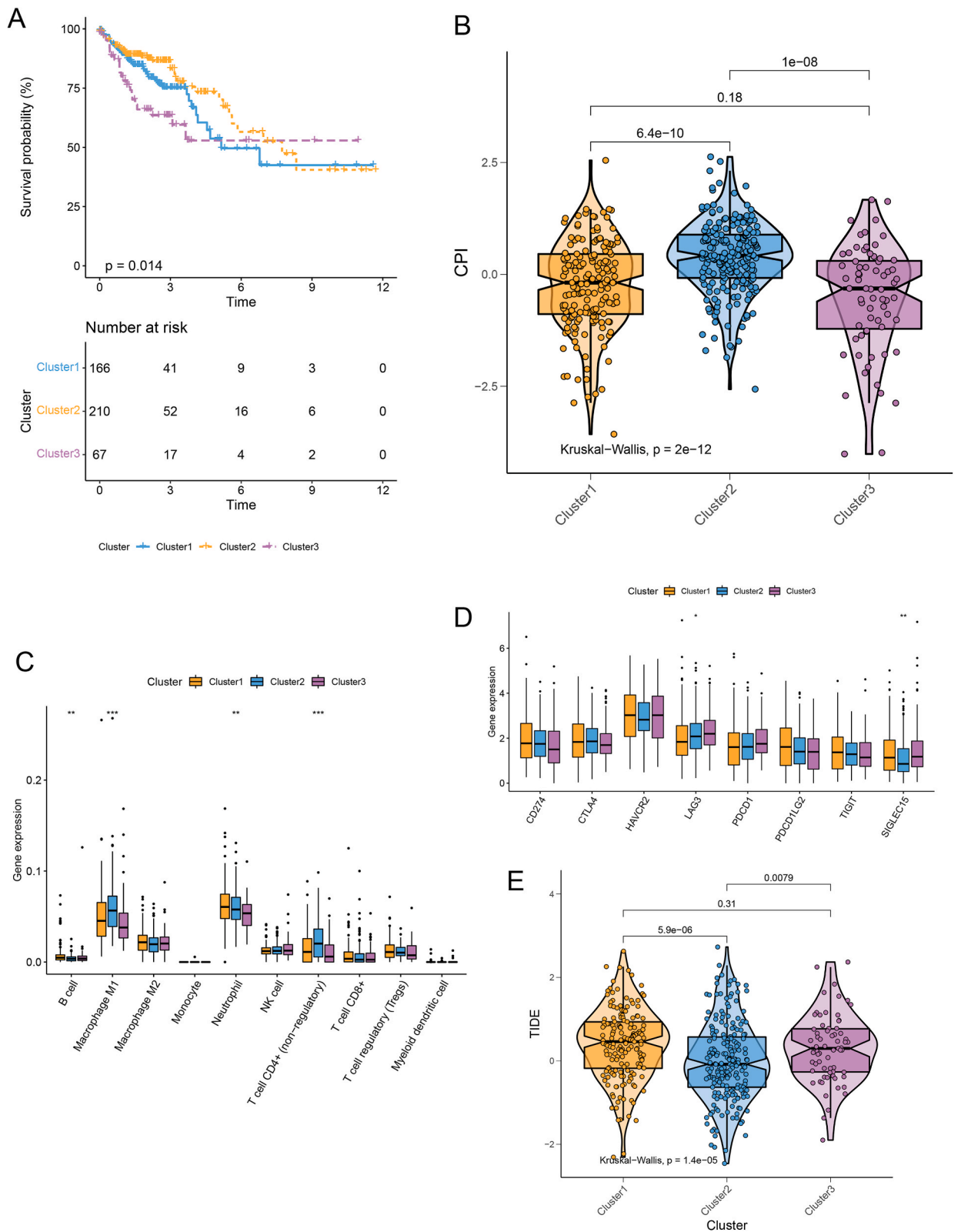


Fig. 7. The differences between the three subtypes in COAD. (A) The difference of OS among the three subtypes. (B) The difference in CPI among the three subtypes. (C) The difference in immune cell infiltration among the three subtypes. (D) The difference in immune checkpoint expression among the three subtypes. (E) The difference in immune efficacy among the three subtypes.

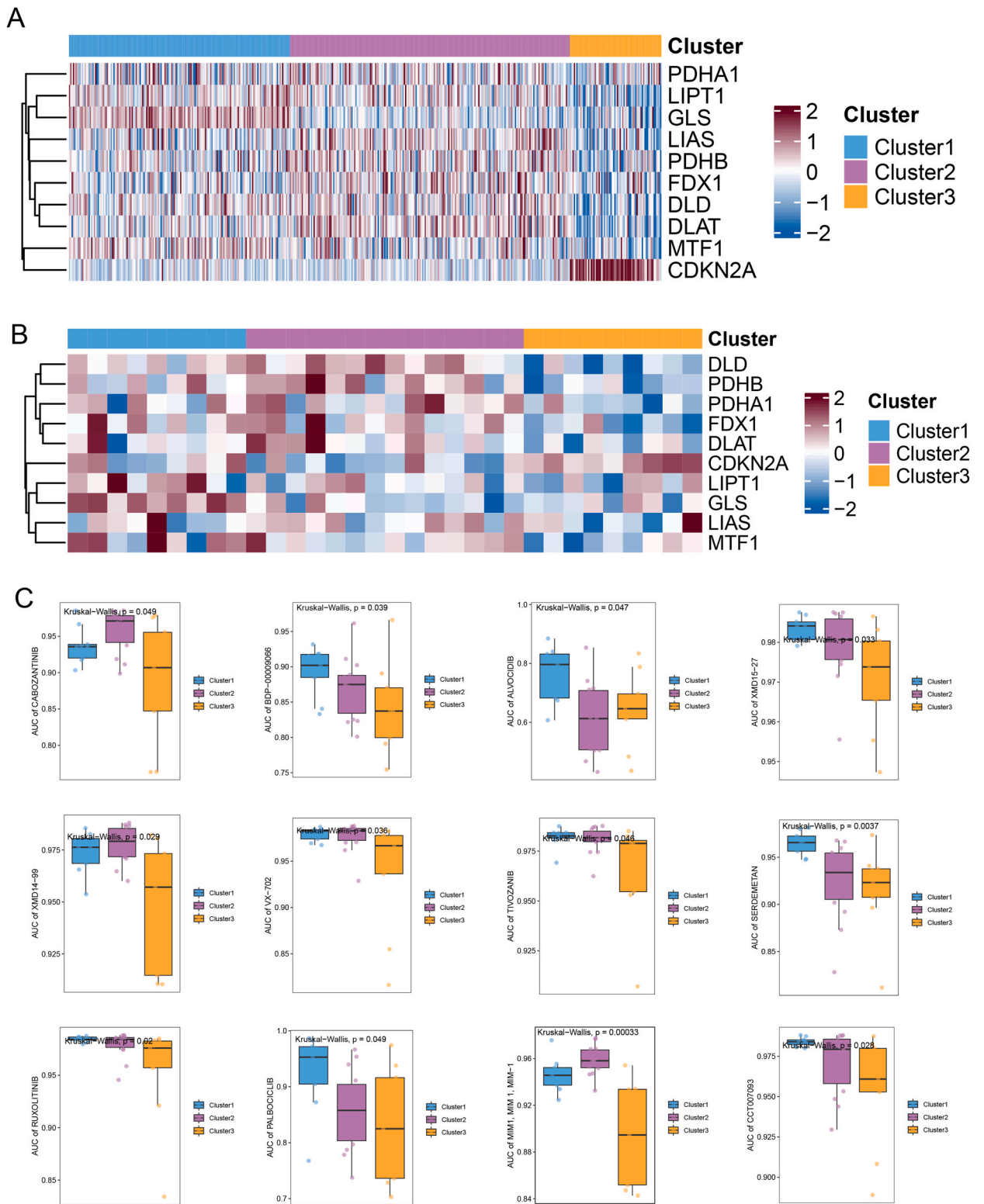


Fig. 8. Expression of CRGs and the difference of drug sensitivity in subtypes. (A) The heatmap of CRGs expression in different subtypes of COAD tissues. (B) The heatmap of CRGs expression in different subtypes of COAD cell lines. (C) The difference in drug sensitivity among subtypes.

3.11. The analysis of drug sensitivity in patients with COAD based on risk score

Of the 138 chemotherapeutic drugs analysed, 17 drugs showed differences in the high- and low-risk groups, namely BI.D1870, BAY.61.3606, BMS.708163, methotrexate, and epothilone. B, AICAR, cisplatin, ATRA, docetaxel, doxorubicin, mitomycin. C, PAC.1, PF.4708671, vinorelbine, JNK.Inhibitor.VIII, pazopanib, camptothecin, and common chemotherapeutic drugs, such as cisplatin, docetaxel, and doxorubicin all showed higher sensitivity in the low-risk group (IC50 was lower), indicating that COAD patients in the low-risk group were more suitable for chemotherapy (Fig. S4).

3.12. Cluster analysis

A consistent cluster divided COAD into three subtypes (k = 3 was the most suitable). Fig. S5 A and B represent the cumulative distribution function (CDF) curve and CDF Delta area curve, respectively, and the delta area curve of the consistent cluster indicates that compared with k = 1, the change in the area under the CDF curve relative to each category number k. Fig. S5C shows the sample distribution map when k = XX and Fig. S5D is the heat map of consistent cluster results when k = XX.

There were survival differences among the three subtypes, with cluster 3 having a shorter OS (Fig. 7A). There were also differences in CPI among the subtypes, with cluster 2 having a higher CPI (Fig. 7B). Regarding immune cell infiltration, B cells, M1 macrophages, neutrophils, and CD4 T cells differed among the three subtypes, and the degree of immune cell infiltration was significantly higher in

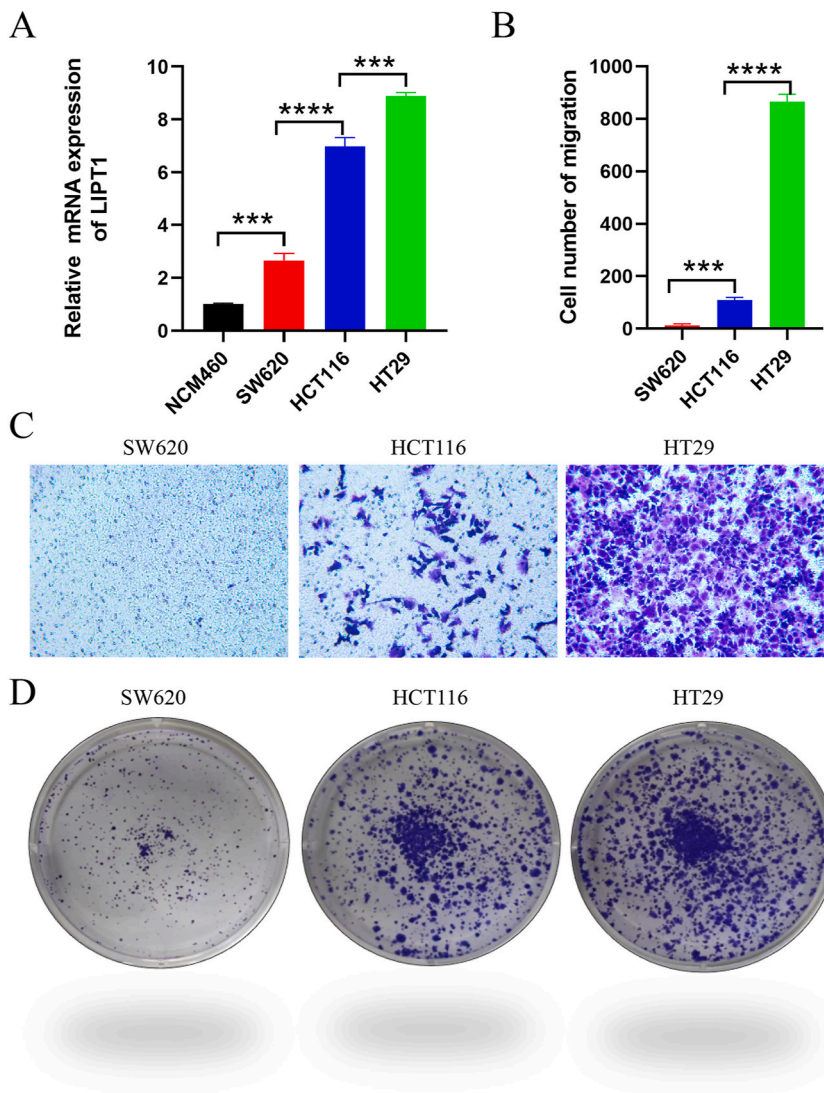


Fig. 9. The Results of cytological verification. (A) The relative mRNA expression of LIPT1. (B) The statistical result of Transwell assay. (C/D) The results of transwell and clone assays.

cluster1 than in the other two subtypes (Fig. 7C). Among the immune checkpoints, SIGLEC1 was highly expressed in cluster1 and cluster3, and LAG3 was highly expressed in cluster3 (Fig. 7D). Regarding the immunotherapy response, cluster1 and cluster3 had higher TIDE scores, and cluster1 and cluster3 were more sensitive to immunotherapy (Fig. 7E).

3.13. The level of CRGs and the drug sensitivity in subtypes of COAD

We used a heat map to show the expression of CRGs in different subtypes of COAD and found that only CDKN2A was significantly overexpressed in cluster3, and FDX1 was significantly overexpressed only in cluster2 (Fig. 8A). The nearest centroid classifier was constructed, and the classifier was used to predict the COAD cell line data in GDSC, which were then divided into three groups according to the COAD typing results. The expression of CRGs in different subtypes of COAD cell lines was displayed with a heat map. This was consistent with the expression of CRGs in tissues (Fig. 8B). Based on the analysis of the relationship between COAD subtypes and drug sensitivity, we found that 12 drugs, including MIM-1, SERDEMETAN, RUXOLITINIB, CCT007093, XMD14-99, XMD15-27, VX-702, BDP-00009066, TIVOZANIB, ALVOCIDIB, CABOZANTINIB, and PALBOCICLIB, were different among the three subtypes, and the AUC was generally higher in cluster2 (Fig. 8C).

3.14. The cytological verification via clone and transwell assays

LIPT1 was positively correlated with the risk score of patients with COAD. To analyse the association between LIPT1 mRNA levels and the malignancy of colon cancer cells, we chose one normal colon cell line (NCM460) and three colon cancer cell lines (SW620, HCT116, and HT29) for PCR, cloning, and transwell assays. The results revealed that the higher the expression of LIPT1 mRNA, the stronger the proliferation and migration of colon cancer cells (Fig. 9). Thus, LIPT1 is a new prospective target for COAD treatment.

4. Discussion

According to the findings of the 2019 Global Burden of Diseases, Injuries, and Risk Factors Study, we understand that cancer-related fatalities rank second globally, coming right after cardiovascular diseases in terms of mortality rates [3]. COAD is the most common malignancy and is also considered one of the major killers of humans [9,33]. Influenced by westernisation, the incidence rate of COAD is high in developed countries and the incidence rate is rising in low- and middle-income countries [34,35]. For the most part, drug resistance, tumour metastasis, and the economic burden of cancer treatment are becoming huge, and the development of cancer more effective treatment remains a great challenge [36,37]. Therefore, it is important to identify more effective indicators for early detection, prognostic judgment, and more effective treatment targets to further improve the outcomes of cancer patients.

Cuption, a study found a new form of cell death, is distinct from all other known cell types, including apoptosis, ferroptosis, pyroptosis, and necroptosis [10]. The main mechanism of cuproptosis involves the accumulation of copper ions in the cells and excessive intracellular copper binding to lipoylated proteins in the tricarboxylic acid (TCA) cycle of the mitochondrial respiratory chain [10,13]. Recent studies have indicated that cuproptosis-related genes or long non-coding RNAs could determine the prognosis and immune cell infiltration in KIRC, LICH, soft tissue sarcomas, and melanoma [18–21]. However, no relevant study has investigated the correlation among CRGs, pan-cancer, and COAD. This study systematically analysed the relationship between CRGs, pan-cancer, and COAD in the present study by comprehensively accessing and analysing public databases.

This study found that CDKN2A was highly expressed in pan-cancer, and almost all of the other nine genes showed low expression in the tumour groups. In a previous study, we found that FDX1, LIPT1, LIAS, DLD, PDHA1, PDHB, and DLAT are positively regulated genes, while MTF1, GLS, and CDKN2A are negatively regulated genes in cuproptosis [10]. Thus, the results indicated that positively regulated CRGs usually had lower expression, whereas negatively regulated CRGs had higher expression in cancer tissues. Our study also found that FDX1 is a protective prognostic factor in LICH and KIRC, while it is a risk factor in LGG. CDKN2A acts as a risk factor in LICH, KIRC, THCA, KICH, and ACC, but acts as a protective factor in HNSC. Therefore, CRGs can serve as a potential pan-cancer prognostic signature. However, the specific mechanism of action of CRGs remains unclear and requires further verification through *in vivo* and *in vitro* experiments.

Several studies have indicated that CRGs are associated with the prognosis and malignancy of many cancers. For example, FDX1 promotes ATP production and is associated with glucose metabolism, fatty acid oxidation, and amino acid metabolism. Zhang found that the level of FDX1 could predict the prognosis of LUAD by mediating metabolism [31]. LIPT1 activates 2-ketoacid dehydrogenases associated with the TCA cycle [38]. One study indicated that higher LIPT1 expression is associated with longer overall survival in melanoma patients than in those with lower LIPT1 expression after receiving immunotherapy. LIPT1 is highly expressed in melanoma biopsies and is an independent favourable prognostic marker for melanoma patients. Furthermore, LIPT1 expression was positively associated with PD-L1 expression but negatively correlated with Treg cell infiltration [20]. The lower the expression of PDHB, the worse the overall survival of patients with NSCLC [39]. DLAT enhances NSCLC cell malignancy by promoting glycolysis and suppressing acetyl-CoA production. Clinically, the higher the DLAT expression, the poorer the prognosis and the higher the SUVmax values on 18F-FDG-PET/CT scans in patients with NSCLC [40]. CDKN2A is a susceptibility gene for pancreatic cancer [41]. CDKN2A is a negative regulator of the cell cycle that plays a role in lethal pancreatic ductal adenocarcinoma [41]. One study also found that CDKN2A could be used as a predictor of haematogenous metastasis in gastric carcinoma [42]. The biotin and lipoic acid synthetase families are encoded by the LISA gene, which is localised in the mitochondria. The final step in the *de novo* pathway for lipoic acid biosynthesis is catalysed by an iron-sulfur enzyme, which is a potent antioxidant [43]. There are no related studies on the correlation between LIAS and cancer. However, the specific mechanisms of action of CRGs in tumourigenesis remain unclear.

Furthermore, we also investigated immune infiltration in pan-cancer tissues and found that CPI positively correlates with immune cells such as nTregs, effector memory cells, neutrophils, Th1 cells, and DC. The level of immune cell infiltration can be used to predict the clinical prognosis of patients. Our study on COAD showed that the higher the immune cell infiltration level, the better the prognosis. In our study, we analysed the essential genes associated with cuproptosis, namely FDX1 and CDKN2A. Our findings revealed a positive correlation between FDX1 and T cell regulation, as well as a positive correlation between CDKN2A and T cell CD4⁺ memory resting. The specific mechanisms by which these two genes influence immune cell infiltration need to be verified through detailed experiments at a later stage. Other studies have found that the expression of CDKN2A is positively associated with the infiltrating levels of B cells, CD8⁺ T cells, CD4⁺ T cells, macrophages, neutrophils, and dendritic cells in hepatocellular carcinoma and that CDKN2A could be used as a prognostic biomarker for determining prognosis and immune infiltration in HCC [44]. CDKN2A loss-of-function negatively affects clinical outcomes in advanced NSCLC patients treated with immune checkpoint blockade, even in high PD-L1 and TMB tumours [45].

Therapeutic methods vary according to tumour sites, such as surgery, chemotherapy, radiotherapy, immunotherapy, and targeted therapy, and have exerted strong efficacy in clinical practice, especially targeted therapy [4–7,46,47]. However, conventional targeted therapies often suffer from severe off-target effects because most critical target facets of cells are shared by all rapidly proliferating cells [17]. The development of new therapeutic agents should aim to increase selectivity and reduce side effects [17]. In recent decades, ferroptosis has emerged as a newly discovered form of cell death regulation. Ferroptosis inducers (including small molecules and nanomaterials) for cancer therapy have made great progress in research [48–51]. Thus, we can design cuproptosis inducers to treat cancer patients in the future.

In addition, our study found that CDKN2A was significantly positively correlated with all drug susceptibilities obtained from the TOP30 drugs in the GDSC database. In contrast, LIAS was significantly negatively correlated with almost all drug susceptibilities obtained from the TOP30 drugs in the CTRP database. Thus, CDKN2A and LIAS expression levels can predict the direction of clinical medication for pan-cancer therapy.

In our study, we constructed a prognostic risk model that included four CRGs in COAD and divided the patients into high- and low-risk groups. The relationship between the risk score and prognosis, immune-related signatures, and drug sensitivity was analysed in COAD. The low-risk group had a better prognosis. The immune infiltration indicators of M1 macrophages, neutrophils, CD4⁺ T cell, and T cell regulation were significantly higher in the low-risk group. Among the immune checkpoints, SIGLEC15 was significantly overexpressed in the high-risk group, and CD274 (PD-L1) was significantly overexpressed in the low-risk group. We used the TIDE website to evaluate the response of the risk model to immunotherapy and then used the IMvigor210 immunotherapy cohort to validate the predictive effect of immunotherapy in this risk model. We found that the high-risk group was more responsive to immunotherapy and had longer OS for the patients who received immunotherapy. The ratio of CR/PR was higher. We also analysed 138 chemotherapeutic drugs and found that 17 drugs (including the common chemotherapeutic drugs cisplatin, docetaxel, and doxorubicin) showed a difference in the high- and low-risk groups, and all had higher sensitivity in the low-risk group. Thus, we concluded that the high-risk group had worse overall survival but more sensitivity to immunotherapy, while the low-risk group had better overall survival and more sensitivity to chemotherapy. Thus, the risk model could predict the prognosis, immune infiltration, and direction of clinical medication in patients with COAD. In addition, the risk model played an important role in the prognosis, immune infiltration, and drug sensitivity among the COAD subgroups.

Our study has several important advantages. First, this is the first study to investigate the association between CRGs, pan-cancers, and COAD. Second, we constructed a new prognostic risk model for cuproptosis in patients with COAD. The risk model can predict prognosis, immune infiltration level, and direction of clinical medication.

Our study also had certain limitations. Firstly, the data of pan-cancer patients regarding the expression levels of CRGs were only evaluated in the TCGA dataset. Therefore, other databases should also be included. Although LIPT1 is a new prospective target for the treatment of patients with COAD, the underlying mechanism remains unclear. The specific mechanism of LIPT1 should be investigated *in vivo* and *in vitro* using the GSEA results as a guide. Besides, the potential mechanism about the 10 genes of CRGs in the development of pan-cancer should be explored in the future and find the difference among pan-cancer about CRGs.

5. Conclusion

In summary, CRGs can be used as potential prognostic biomarkers to predict immune infiltration levels in patients with pan-cancer. In addition, the risk model could more accurately predict the prognosis and immune infiltration levels of patients with COAD and better guide the direction of clinical medication. Besides, FDX1, CDKN2A, and LIPT1 may serve as prospective new targets for cancer therapy.

Ethics statement

No applicable.

Data availability statement

All the data supporting the findings of this study are available within the main text of this article and its Supplementary Information. Source data are provided with this paper.

Funding

This work was supported by the National Natural Science Foundation of China (Grant No. 82002433), the Collaborative Innovation Major Project of Zhengzhou (Grant No. 20XTZX08017), the Science and Technology Project of Henan Provincial Department of Education (Grant No. 21A320036), Young and Middle-aged Health Science and Technology Innovation Talents in 2020 (Grant No. YXKC2020049), Henan Province Medical Science and Technology Research Project Joint Construction Project (Grant No. LHGJ20190003, LHGJ20190055) and State Key Laboratory of Pathogenesis, Prevention, and Treatment of High Incidence Diseases in Central Asia Fund (SKL-HIDCA-2022- JZ5)

CRediT authorship contribution statement

Chunwei Li: Data curation. **Lili Zhu:** Writing – original draft. **Qinghua Liu:** Formal analysis. **Mengle Peng:** Formal analysis. **Jinhai Deng:** Formal analysis. **Zhirui Fan:** Writing – review & editing. **Xiaoran Duan:** Writing – review & editing. **Ruyue Xue:** Writing – review & editing. **Zhiping Guo:** Validation. **Xuefeng Lv:** Validation. **Lifeng Li:** Funding acquisition. **Jie Zhao:** Funding acquisition.

Declaration of competing interest

All authors stated that there is no conflict of interest in this article.

Acknowledgments

We want to thank the public database and those who assisted in the study.

Appendix A. Supplementary data

Supplementary data to this article can be found online at <https://doi.org/10.1016/j.heliyon.2024.e34011>.

References

- [1] C. Wu, M. Li, H. Meng, et al., Analysis of status and countermeasures of cancer incidence and mortality in China, *Sci. China Life Sci.* 62 (2019) 640–647.
- [2] R.L. Siegel, K.D. Miller, H.E. Fuchs, A. Jemal, Cancer statistics, 2022, *CA A Cancer J. Clin.* 72 (2022) 7–33.
- [3] C. Global Burden of Disease Cancer, J.M. Kocarnik, K. Compton, et al., Cancer incidence, mortality, years of life lost, years lived with disability, and disability-adjusted life years for 29 cancer groups from 2010 to 2019: a systematic analysis for the global burden of disease study 2019, *JAMA Oncol.* 8 (2022) 420–444.
- [4] M. Burotto, J. Wilkerson, W.D. Stein, et al., Adjuvant and neoadjuvant cancer therapies: a historical review and a rational approach to understand outcomes, *Semin. Oncol.* 46 (2019) 83–99.
- [5] S. Apuri, Neoadjuvant and adjuvant therapies for breast cancer, *South. Med. J.* 110 (2017) 638–642.
- [6] R. Hernandez, J. Poder, K.M. LaPorte, T.R. Malek, Engineering IL-2 for immunotherapy of autoimmunity and cancer, *Nat. Rev. Immunol.* 22 (2022) 614–628.
- [7] S. Cafarotti, F. Lococo, P. Froesh, et al., Target therapy in lung cancer, *Adv. Exp. Med. Biol.* 893 (2016) 127–136.
- [8] R. Labianca, G.D. Beretta, B. Kildani, et al., Colon cancer, *Crit. Rev. Oncol. Hematol.* 74 (2010) 106–133.
- [9] A. Recio-Boiles, B. Cagir, Colon cancer, in: *StatPearls*, Treasure Island (FL), 2022.
- [10] P. Tsvetkov, S. Coy, B. Petrova, et al., Copper induces cell death by targeting lipoylated TCA cycle proteins, *Science* 375 (2022) 1254–1261.
- [11] Y. Wang, L. Zhang, F. Zhou, Cuproptosis: a new form of programmed cell death, *Cell. Mol. Immunol.* 19 (2022) 867–868.
- [12] P.A. Cobine, D.C. Brady, Cuproptosis: cellular and molecular mechanisms underlying copper-induced cell death, *Mol. Cell* 82 (2022) 1786–1787.
- [13] S.R. Li, L.L. Bu, L. Cai, Cuproptosis: lipoylated TCA cycle proteins-mediated novel cell death pathway, *Signal Transduct. Targeted Ther.* 7 (2022) 158.
- [14] D. Tang, X. Chen, G. Kroemer, Cuproptosis: a copper-triggered modality of mitochondrial cell death, *Cell Res.* 32 (2022) 417–418.
- [15] E.J. Ge, A.I. Bush, A. Casini, et al., Connecting copper and cancer: from transition metal signalling to metalloplasia, *Nat. Rev. Cancer* 22 (2022) 102–113.
- [16] P.A. Cobine, S.A. Moore, S.C. Leary, Getting out what you put in: copper in mitochondria and its impacts on human disease, *Biochim. Biophys. Acta Mol. Cell Res.* 1868 (2021) 118867.
- [17] V. Oliveri, Selective targeting of cancer cells by copper ionophores: an overview, *Front. Mol. Biosci.* 9 (2022) 841814.
- [18] Z. Bian, R. Fan, L. Xie, A novel cuproptosis-related prognostic gene signature and validation of differential expression in clear cell renal cell carcinoma, *Genes* 13 (2022).
- [19] G.S.J. Zhang, X. Zhang, A novel Cuproptosis-related lncRNA signature to predict prognosis in hepatocellular carcinoma, *Sci. Rep.* 12 (11) (2022 Jul 5) 11325.
- [20] H. Lv, X. Liu, X. Zeng, et al., Comprehensive analysis of cuproptosis-related genes in immune infiltration and prognosis in melanoma, *Front. Pharmacol.* 13 (2022) 930041.
- [21] J. Han, Y. Hu, S. Liu, et al., A newly established cuproptosis-associated long non-coding RNA signature for predicting prognosis and indicating immune microenvironment features in soft tissue sarcoma, *J Oncol* 2022 (2022) 8489387.
- [22] M. Yang, H. Zheng, K. Xu, et al., A novel signature to guide osteosarcoma prognosis and immune microenvironment: cuproptosis-related lncRNA, *Front. Immunol.* 13 (2022) 919231.
- [23] Z. Zhang, X. Zeng, Y. Wu, et al., Cuproptosis-related risk score predicts prognosis and characterizes the tumor microenvironment in hepatocellular carcinoma, *Front. Immunol.* 13 (2022) 925618.
- [24] L. Yang, J. Yu, L. Tao, et al., Cuproptosis-related lncRNAs are biomarkers of prognosis and immune microenvironment in head and neck squamous cell carcinoma, *Front. Genet.* 13 (2022) 947551.
- [25] Z.H. Ji, W.Z. Ren, H.Q. Wang, et al., Molecular subtyping based on cuproptosis-related genes and characterization of tumor microenvironment infiltration in kidney renal clear cell carcinoma, *Front. Oncol.* 12 (2022) 919083.
- [26] B. Chen, X. Zhou, L. Yang, et al., A Cuproptosis Activation Scoring model predicts neoplasm-immunity interactions and personalized treatments in glioma, *Comput. Biol. Med.* 148 (2022) 105924.

- [27] Y.J. Li, H.Y. Li, Q. Zhang, S.L. Wei, The prognostic value and immune landscape of a cuproptosis-related lncRNA signature in head and neck squamous cell carcinoma, *Front. Genet.* 13 (2022) 942785.
- [28] X. Mo, D. Hu, P. Yang, et al., A novel cuproptosis-related prognostic lncRNA signature and lncRNA MIR31HG/miR-193a-3p/TNFRSF21 regulatory axis in lung adenocarcinoma, *Front. Oncol.* 12 (2022) 927706.
- [29] Y. Zhou, Q. Shu, Z. Fu, et al., A novel risk model based on cuproptosis-related lncRNAs predicted prognosis and indicated immune microenvironment landscape of patients with cutaneous melanoma, *Front. Genet.* 13 (2022) 959456.
- [30] Y. Yun, Y. Wang, E. Yang, X. Jing, Cuproptosis-related gene - SLC31A1, FDX1 and ATP7B - polymorphisms are associated with risk of lung cancer, *Pharmacogenomics Pers Med* 15 (2022) 733–742.
- [31] Z. Zhang, Y. Ma, X. Guo, et al., FDX1 can impact the prognosis and mediate the metabolism of lung adenocarcinoma, *Front. Pharmacol.* 12 (2021) 749134.
- [32] H.I. Khouja, I.M. Ashankyty, L.H. Bajrai, et al., Multi-staged gene expression profiling reveals potential genes and the critical pathways in kidney cancer, *Sci. Rep.* 12 (2022) 7240.
- [33] C. Xia, X. Dong, H. Li, et al., Cancer statistics in China and United States, 2022: profiles, trends, and determinants, *Chin Med J (Engl)* 135 (2022) 584–590.
- [34] H. Birgisson, E.J. Olafsdottir, A. Sverrisdottir, et al., [Screening for cancer of the colon and rectum A review on incidence, mortality, cost and benefit], *Laeknabladid* 107 (2021) 398–405.
- [35] Y. Xi, P. Xu, Global colorectal cancer burden in 2020 and projections to 2040, *Transl Oncol* 14 (2021) 101174.
- [36] H. Qiu, S. Cao, R. Xu, Cancer incidence, mortality, and burden in China: a time-trend analysis and comparison with the United States and United Kingdom based on the global epidemiological data released in 2020, *Cancer Commun.* 41 (2021) 1037–1048.
- [37] I. Soerjomataram, F. Bray, Planning for tomorrow: global cancer incidence and the role of prevention 2020–2070, *Nat. Rev. Clin. Oncol.* 18 (2021) 663–672.
- [38] A. Solmonson, B. Faubert, W. Gu, et al., Compartmentalized metabolism supports midgestation mammalian development, *Nature* 604 (2022) 349–353.
- [39] P. Giannos, K.S. Kechagias, A. Gal, Identification of prognostic gene biomarkers in non-small cell lung cancer progression by integrated bioinformatics analysis, *Biology* 10 (2021).
- [40] Q. Chen, Y. Wang, L. Yang, et al., PM2.5 promotes NSCLC carcinogenesis through translationally and transcriptionally activating DLAT-mediated glycolysis reprogramming, *J. Exp. Clin. Cancer Res.* 41 (2022) 229.
- [41] H. Kimura, A.P. Klein, R.H. Hruban, N.J. Roberts, The role of inherited pathogenic CDKN2A variants in susceptibility to pancreatic cancer, *Pancreas* 50 (2021) 1123–1130.
- [42] J. Qiao, Y. Tian, X. Cheng, et al., CDKN2A deletion leading to hematogenous metastasis of human gastric carcinoma, *Front. Oncol.* 11 (2021) 801219.
- [43] Y.Z. Zhao, M.Y. Chang, G.C. Xu, et al., [Expression of LIAS and NRF2 in PBMCs from patients with silicosis and their correlation with silicosis], *Zhonghua Lao Dong Wei Sheng Zhi Ye Bing Za Zhi* 39 (2021) 893–898.
- [44] J.P. Luo, J. Wang, J.H. Huang, CDKN2A is a prognostic biomarker and correlated with immune infiltrates in hepatocellular carcinoma, *Biosci. Rep.* 41 (2021).
- [45] S.I. Gutiontov, W.T. Turchan, L.F. Spurr, et al., CDKN2A loss-of-function predicts immunotherapy resistance in non-small cell lung cancer, *Sci. Rep.* 11 (2021) 20059.
- [46] U. Schick, I. Latorzeff, P. Sargos, Postoperative radiotherapy in prostate cancer: dose and volumes, *Cancer Radiother.* 25 (2021) 674–678.
- [47] Z. Al-Hilli, A. Wilkerson, Breast surgery: management of postoperative complications following operations for breast cancer, *Surg. Clin.* 101 (2021) 845–863.
- [48] C. Liang, X. Zhang, M. Yang, X. Dong, Recent progress in ferroptosis inducers for cancer therapy, *Adv. Mater.* 31 (2019) e1904197.
- [49] P. Koppula, L. Zhuang, B. Gan, Cystine transporter SLC7A11/xCT in cancer: ferroptosis, nutrient dependency, and cancer therapy, *Protein Cell* 12 (2021) 599–620.
- [50] N. Zaffaroni, G.L. Beretta, Ferroptosis inducers for prostate cancer therapy, *Curr. Med. Chem.* 29 (2022) 4185–4201.
- [51] G. Lei, L. Zhuang, B. Gan, Targeting ferroptosis as a vulnerability in cancer, *Nat. Rev. Cancer* 22 (2022) 381–396.